

Effect of the configuration interaction on the fine-structure-level splittings for quasi-two-electron atoms

T. N. Chang

Physics Department, University of Southern California, Los Angeles, California 90089-0484

E. T. Bryan

Physics Department, University of California, Riverside, California 92521

(Received 9 October 1987)

A calculational procedure is presented to study the effect of the configuration interaction on the fine-structure-level splittings for a quasi-two-electron atom. A detailed application is carried out to examine the anomaly in the fine-structure-level splittings of the Al II $1,3F$ series which are strongly affected by the presence of the $3p3d\ ^3F$ perturber. Our calculated level splittings are in close agreement with the available experimental values. In particular, our study has identified a direct link between the experimentally observed fine-structure-level splittings and the probability densities of the dominating configuration in the calculated state wave functions.

I. INTRODUCTION

When the nuclear charge Z is not too much larger than the number of atomic electrons N , the spectra of a *quasi-two-electron* atom with two electrons outside a $1S$ core are often described by the LS coupling. The fine-structure-level splitting between singlet and triplet states corresponding to the same configuration is accounted for at least qualitatively by the *electrostatic exchange interaction* between the two outer electrons. In the *absence* of significant configuration mixing, the splittings between three different J levels within a manifold of triplet state of given total orbital angular momentum L is usually represented by the simple *Landé interval rule*,¹ and can be estimated by the first-order perturbation contribution in energy from the spin-dependent magnetic fine-structure interactions with a zeroth-order nonrelativistic wave function.²

In contrast, for states dominated by strong configuration mixing, the fine-structure-level splittings for a specific singlet-triplet complex often deviate significantly from this simple theoretical interpretation. In particular, the level splittings are found to vary substantially from the usual $(n^*)^{-3}$ dependence along a given configuration series. One of the best known examples is the Al II $3snf\ ^3F$ configuration series, which is strongly affected by the presence of a "diluted" $3p3d\ ^3F$ state between $3s6f\ ^3F$

and $3s7f\ ^3F$ states.³⁻⁶ The effect of the configuration interaction to the fine structure of this Al II $3F$ series was examined qualitatively by Weiss³ and subsequently studied quantitatively by Froese Fischer.⁴ Table I summarizes the experimentally observed splittings⁶ between different levels within each $1,3F$ complex. The influence of the configuration interaction due to the $3p3d\ ^3F$ state is clearly illustrated by the presence of the maximum splittings between three $3p3d\ ^3F$ levels and the $1F-3F$ level inversion between $3s6f$ and $3s7f$ states. In addition, the experimental ratio R between the level splittings, i.e., $R = \Delta_3/\Delta_2$, for the $3s7f\ ^3F$ state deviates significantly from the expected value of 0.75 from the Landé interval rule.

In this paper we will present a simple calculational procedure which is computationally effective in the determination of the fine-structure-level splittings for a configuration series strongly disturbed by the presence of a perturber located in the midst of this series for a quasi-two-electron atom. We will examine the numerical accuracy of this theoretical procedure by comparing the calculated fine-structure-level splittings with the available experimental data. In addition, our calculation has established a direct link between the experimental level splitting and the calculated probability density from the dominated contributing configuration. This link makes it possible to extract from the experimental data the infor-

TABLE I. Experimental fine-structure-level splittings in cm^{-1} for Al II $1,3F$ states from Ref. 6.

State	$\Delta_1 = \epsilon(^1F_3) - \epsilon(^3F_3)$	$\Delta_2 = \epsilon(^3F_4) - \epsilon(^3F_3)$	$\Delta_3 = \epsilon(^3F_3) - \epsilon(^3F_2)$	$R = \Delta_3/\Delta_2$
$3s4f$	50.05	2.91	1.97	0.677
$3s5f$	238.70	6.99	5.37	0.768
$3s6f$	706.49	22.9	17.5	0.764
$3p3d$		33.0	25.2	0.764
$3s7f$	-668.81	10.89	7.03	0.646
$3s8f$	-347.48	3.38	2.42	0.716
$3s9f$	-222.29	1.48	1.09	0.736

mation on the relative contribution (or relative spectral purity⁷) of the dominating electronic configuration to the multiconfiguration state wave functions between neighboring states *if* the level splittings for each state in this series are primarily determined by this dominating configuration.

II. THEORY AND CALCULATIONAL PROCEDURE

As we pointed out earlier, when the spectrum of a quasi-two-electron atom is characterized by the *LS* coupling, the singlet-triplet fine-structure splitting is dominated by the electrostatic exchange interaction. Recent works have shown that a nonrelativistic superposition of the configuration wave function method^{5,8,9} (SCW) is capable of estimating quantitatively the *J*-independent term values of the singlet and triplet states to a fairly high degree of accuracy. For the fine-structure splittings between different *J* levels of a triplet state dominated by strong configuration mixing, a detailed theoretical estimation would require an explicit calculation beyond the lowest-order perturbation contribution from spin-dependent magnetic fine-structure interactions.

In the Breit-Pauli approximation,² the magnetic fine-structure interactions responsible for the level splittings for an *N*-electron atom of nuclear charge *Z* can be separated into three terms, i.e., the spin-orbit interaction $H_{s.o.}$, the spin-spin interaction H_{ss} , and the spin-other-orbit interaction $H_{s.o.o.}$. All three interactions are proportional to the square of the fine-structure constant, i.e., α^2 , and the detailed expressions of these three terms in rydbergs are given by^{1,2}

$$H_m = \alpha^2 (H_{s.o.} + H_{ss} + H_{s.o.o.}), \quad (1)$$

where

$$H_{s.o.} = \sum_i \frac{Z}{r_i^3} (\mathbf{l}_i \cdot \mathbf{s}_i), \quad (2)$$

$$H_{ss} = \sum_{\substack{i,j=1 \\ (i \neq j)}}^N \frac{1}{r_{ij}^3} \left[\mathbf{s}_i \cdot \mathbf{s}_j - \frac{3(\mathbf{s}_i \cdot \mathbf{r}_{ij})(\mathbf{s}_j \cdot \mathbf{r}_{ij})}{r_{ij}^2} \right], \quad (3)$$

$$H_{s.o.o.} = \sum_{\substack{i,j=1 \\ (i \neq j)}}^N \frac{1}{r_{ij}^3} (\mathbf{r}_{ij} \times \mathbf{p}_i) \cdot (\mathbf{s}_i + 2\mathbf{s}_j), \quad (4)$$

and $\mathbf{r}_{ij} = \mathbf{r}_j - \mathbf{r}_i$.

In the present calculation, the configuration wave function $\Psi_{n_i l_i, n_j l_j}^{SL}$ in the *LS* representation [e.g., Eq. (3) of Ref. 8] employed in our nonrelativistic SCW procedure will be replaced by a *composite configuration wave function* Ψ^{SLJM} corresponding to total angular momentum *J* and its magnetic component *M*. More specifically, Ψ^{SLJM} is expressed as the sum of Ψ^{SL} over the magnetic quantum numbers M_S and M_L , i.e.,

$$\Psi_{n_i l_i, n_j l_j}^{SLJM} = \sum_{M_S, M_L} (-1)^{L-S} (2J+1)^{1/2} \times \begin{Bmatrix} S & L & J \\ M_S & M_L & M \end{Bmatrix} \Psi_{n_i l_i, n_j l_j}^{SL}. \quad (5)$$

For the nonrelativistic spin-independent part of the Hamiltonian H_{NR} [i.e., Eq. (1) in Ref. 8], the Hamiltonian matrix constructed with Ψ^{SLJM} remains unchanged and is given by the same expression derived from the *LS* configuration wave function Ψ^{SL} [i.e., Eq. (6) in Ref. 8]. Consequently, the *J*-dependent *state wave function* $\Phi_{n_\mu l_\mu, n_\nu l_\nu}^{SLJM}$, designated by its dominating configuration $(n_\mu l_\mu, n_\nu l_\nu)$, is calculated with the same nonrelativistic SCW procedure^{8,9} with Ψ^{SL} replaced by Ψ^{SLJM} , i.e.,

$$\Phi_{n_\mu l_\mu, n_\nu l_\nu}^{SLJM} = \sum_{n_i l_i, n_j l_j} C_{\mu\nu}^{SL}(n_i l_i, n_j l_j) \Psi_{n_i l_i, n_j l_j}^{SLJM}, \quad (6)$$

where $|C_{\mu\nu}^{SL}(n_i l_i, n_j l_j)|^2$ is the probability density (or spectral purity) corresponding to the $(n_i l_i, n_j l_j)$ configuration.

With this choice of *zeroth-order-state wave function* $\Phi_{n_\mu l_\mu, n_\nu l_\nu}^{SLJM}$ in the *J* representation, the fine-structure-level splittings can be evaluated with the following procedure. First, we construct a new Hamiltonian matrix with respect to the zeroth-order-state wave functions Φ^{SLJM} by including the spin-dependent magnetic interactions in the total Hamiltonian *H*, i.e.,

$$H = H_{NR} + H_m. \quad (7)$$

Since the nonrelativistic part of the Hamiltonian, i.e., H_{NR} , is already diagonalized with respect to the zeroth-order-state wave functions, no additional calculation is required. The Hamiltonian matrix element for H_m is given by

$$\langle \Phi_{n_\sigma l_\sigma, n_\lambda l_\lambda}^{S'L'J'M'} | H_m | \Phi_{n_\xi l_\xi, n_\zeta l_\zeta}^{SLJM} \rangle = \delta_{J'J} \delta_{M'M} \sum_{\alpha, \beta, \mu, \nu} C_{\sigma\lambda}^{S'L'}(n_\alpha l_\alpha, n_\beta l_\beta) C_{\xi\zeta}^{SL}(n_\mu l_\mu, n_\nu l_\nu) \langle \Psi_{n_\alpha l_\alpha, n_\beta l_\beta}^{S'L'J'M'} | H_m | \Psi_{n_\mu l_\mu, n_\nu l_\nu}^{SLJM} \rangle, \quad (8)$$

where the sum includes all configuration combinations. For each *J* value, the Hamiltonian matrix for the Hamiltonian *H* in the *J* representation is constructed by including all $(nl, n'l')$ *SLJ* states which are mixed through configuration interaction for *all allowed* $(nl, n'l')$ *SL* combinations. Second, we calculate the energy eigenvalues and their corresponding eigenvectors by diagonalizing the new Hamiltonian matrix. This step is repeated for

each *J* state. Finally, we evaluate the level splittings by taking the energy difference between the energy eigenvalues of different *J* states.

We now turn our attention to the calculation of matrix elements with respect to the *J*-dependent configuration wave functions Ψ^{SLJ} for the spin-dependent part of the Hamiltonian, i.e., the spin-orbit interaction $H_{s.o.}$, the spin-spin interaction H_{ss} , and the spin-other-orbit in-

teraction $H_{s.o.o.}$. Similar to the nonrelativistic procedure, our derivation will be limited to the two outermost electrons in a frozen-core approximation.

The analytical expression of the matrix element for the

spin-orbit interaction $H_{s.o.}$ can be evaluated following a straightforward application of the Wigner-Eckart theorem to the scalar product of two tensor operators of rank 1, i.e.,

$$\langle \Psi_{n_\alpha l_\alpha, n_\beta l_\beta}^{S'L'J'M'} | H_{s.o.} | \Psi_{n_\mu l_\mu, n_\nu l_\nu}^{SLJM} \rangle = \delta_{J'J} \delta_{M'M} (-1)^{l_\alpha + l_\beta + S' + S + J + 1} \rho(L'S', LS, J) \\ \times [V(\alpha, \beta, \mu, \nu) + (-1)^\Delta V(\beta, \alpha, \mu, \nu) + (-1)^\Delta V(\alpha, \beta, \nu, \mu) + (-1)^{\Delta + \Delta'} V(\beta, \alpha, \nu, \mu)], \quad (9)$$

where

$$\Delta = l_\mu + l_\nu - L - S, \quad (10)$$

$$\Delta' = l_\alpha + l_\beta - L' - S', \quad (11)$$

$$\rho(L'S', LS, J) = \left(\frac{3}{2}\right)^{1/2} [(2L' + 1)(2S' + 1)(2L + 1)(2S + 1)]^{1/2} \begin{Bmatrix} L' & L & 1 \\ S & S' & J \end{Bmatrix} \begin{Bmatrix} \frac{1}{2} & \frac{1}{2} & 1 \\ S & S' & \frac{1}{2} \end{Bmatrix}, \quad (12)$$

$$V(\alpha, \beta, \mu, \nu) = \delta_{l_\beta l_\nu} \delta_{l_\alpha l_\mu} [(2l_\mu + 1)(l_\mu + 1)l_\mu]^{1/2} \begin{Bmatrix} L' & L & 1 \\ l_\mu & l_\mu & l_\nu \end{Bmatrix} \langle n_\alpha l_\alpha | v | n_\mu l_\mu \rangle \langle \chi_{n_\beta l_\beta} | \chi_{n_\nu l_\nu} \rangle, \quad (13)$$

and

$$\langle nl | v | n'l' \rangle = \int dr \chi_{nl}(r) (Z/r^3) \chi_{n'l'}(r) \quad (14)$$

is the one-particle integral over the radial part of the spin-orbit interaction. The radial part of the one-particle orbit wave function χ is generated with the one-electron radial *Hartree-Fock* Hamiltonian h^{HF} constructed with the Ne-like 1S frozen Hartree-Fock core of $N-2$ electrons. [The detailed expression of h^{HF} is given by Eq. (7) in Ref. 8.]

For the spin-spin and spin-other-orbit interactions, an early attempt was made by Marvin¹⁰ to derive a general analytical expression for the matrix element between two arbitrary two-electron configurations in a straightforward application of the angular momentum algebra. The procedure employed by Marvin is extremely tedious and only a limited number of matrix elements between configurations of lower- l orbits are given explicitly. The extension to other configurations involving orbits of higher- l values would require even more effort than that of Marvin. In addition, a trivial error in the unsymmetrical form of the spin-other-orbit term employed by Marvin has led to incorrect results to his calculations, except for matrix elements between configuration of two equivalent electrons. In the present calculation, analytical expressions for the matrix elements of spin-spin and spin-other-orbit interactions are derived with the help of a more compact tensorial operator technique developed by Judd.¹¹

For the spin-spin interaction, in a very elegant application of tensor algebra, Judd¹¹ has shown that the spin-spin interaction can be expressed in terms of the sum of scalar products of tensors of rank 2 which are in turn the tensor products of spherical harmonics $C^{(k)}$ and spin angular momentum operators $s^{(1)}$. More specifically, following the derivation of Judd,¹¹ the spin-spin interaction can be written as

$$H_{ss}(1,2) = -\frac{1}{2} \sum_k \left[\frac{(2k+5)!}{(2k)!} \right]^{1/2} \\ \times [\Theta(r_2 - r_1) Q_{12}(k; k, k+2) \\ + \Theta(r_1 - r_2) Q_{12}(k; k, +2, k)], \quad (15)$$

where

$$Q_{ij}(k; \mu, \nu) = (-1)^k \frac{r_i^k}{r_j^{k+3}} [[C^{(\mu)}(i) \times C^{(\nu)}(j)]^{(2)} \\ \times [s_i^{(1)} \times s_j^{(1)}]^{(2)}]^{(0)} \quad (16)$$

and

$$\Theta(r_i - r_j) = \begin{cases} 1, & r_i > r_j \\ 0, & r_i < r_j \end{cases} \quad (17)$$

With the spin-spin interaction expressed as a scalar product of tensor operators of rank 2, the matrix elements between configuration wave functions in J representation can be derived analytically following a straightforward application of the Wigner-Eckart theorem. The explicit expression for this matrix elements will be given in the Appendix.

To calculate the matrix elements of the spin-other-orbit interaction between two arbitrary configuration wave functions in the J representation, we rewrite the expression given in Eq. (4) into a sum of scalar products of tensor operators following a procedure similar to the one employed by Judd.¹¹ First, we separate the $H_{s.o.o.}$ term into two parts, i.e.,

$$H_{s.o.o.}(1,2)=[h(1,2)+h(2,1)], \quad (18)$$

where

$$h(i,j)=\frac{\mathbf{r}_{ij}}{r_{ij}^3} \times \mathbf{p}_i \cdot (\mathbf{s}_i + 2\mathbf{s}_j). \quad (19)$$

The next step is to express \mathbf{r}_{ij} , r_{ij}^{-3} , and \mathbf{p}_i in terms of the tensor operators of the spherical harmonic $C^{(k)}$, i.e.,

$$\mathbf{r}_{ij}=r_j C^{(1)}(j)-r_i C^{(1)}(i), \quad (20)$$

$$h(i,j)=\sum_{k=0}^{\infty} (-1)^k \left[\left(\frac{2k+3}{3} \right)^{1/2} \{ \Theta(r_j-r_i)[(k+2)U_{ij}(k-1;k+1,k+1)+(2k+5)U_{ij}(k;k+2,k+1)] \right. \\ \left. - \Theta(r_i-r_j)[(k+1)U_{ij}(k+1;k+1,k+1)+(2k+1)U_{ij}(k;k,k+1)] \right] \\ + \left[\frac{k(k+1)(2k+1)}{3} \right]^{1/2} [\Theta(r_j-r_i)W_{ij}(k-1,k) + \Theta(r_i-r_j)W_{ij}(k,k)], \quad (23)$$

where

$$U_{ij}(k;\nu,\mu)=\frac{r_{<}^k}{r_{>}^{k+3}} [[C^{(\nu)}(j) \times [C^{(\nu)}(i) \times I^{(1)}(i)]^{(\mu)}]^{(1)} \\ \times [s_i^{(1)} + 2s_j^{(1)}]^{(0)} \quad (24)$$

and

$$W_{ij}(k,\nu)=\frac{r_{<}^k}{r_{>}^{k+2}} [[C^{(\nu)}(j) \times C^{(\nu)}(i)]^{(1)} \\ \times [s_i^{(1)} + 2s_j^{(1)}]^{(0)} \left[\frac{\partial}{\partial r_i} \right]. \quad (25)$$

A similar, but less compact expression was also derived by Blume and Watson.¹² With the spin-other-orbit interaction now expressed in terms of a sum of scalar products of tensor operators, again, the matrix elements calculation becomes a simple application of the Wigner-Eckart theorem and its explicit expression will also be given in the Appendix.

III. APPLICATION AND DISCUSSIONS

To illustrate the effectiveness of the calculational procedure outlined in Sec. II and to examine the anomaly in the fine-structure-level splittings due to the effect of the configuration interaction in a quasi-two-electron atom, we have carried out a detailed fine-structure calculation for the Al II $1,3F$ states. Our numerical calculation starts with the construction of the *zeroth-order state wave functions* following the nonrelativistic SCW procedure employed in our previous calculation.⁵

Similar to our earlier calculations,^{5,8,9} we have limited the configurations included in our study to those with

$$r_{ij}^{-3}=\sum_{k=0}^{\infty} (-1)^k (2k+1)^{3/2} [C^{(k)}(i) \times C^{(k)}(j)]^{(0)} \\ \times \left[\sum_{v=0}^{\infty} \frac{r_{<}^{k+2v}}{r_{>}^{k+3+2v}} \right], \quad (21)$$

and

$$\mathbf{p}_i=i2^{1/2}r_i^{-1}[C^{(1)}(i) \times I^{(1)}(i)]^{(1)}-i\frac{\partial}{\partial r_i}C^{(1)}(i). \quad (22)$$

After a series of recoupling of tensor operators $C^{(k)}$, $I^{(1)}$, and $s^{(1)}$, it can be shown eventually that the term $h(i,j)$ in Eq. (19) can be expressed as a sum of scalar products of tensor operators, i.e.,

two outermost electrons in various two-electron orbitals outside a $1S$ frozen core of $N-2$ electrons shown in Table II. This choice of configuration combinations effectively leaves out the contribution from the core polarization interaction which, in principle, can be included explicitly in the calculation *if* electronic configurations corresponding to *simultaneous* excitation of one outer electron and one inner-shell electron from the $1S$ core are also present in the Hamiltonian matrix calculation. Instead, in our calculation, the core polarization interaction is approximated by adding to the H_{NR} term in Eq. (7) the *dipole polarization interaction* V_α and the *dielectronic potential*¹³ V_d , i.e.,

$$V_\alpha=-\sum_{i=1}^N V_p(r_i), \quad (26)$$

$$V_d=-2 \sum_{\substack{i,j=1 \\ (i \neq j)}}^N (\hat{\mathbf{r}}_i \cdot \hat{\mathbf{r}}_j) [V_p(r_i)V_p(r_j)]^{1/2}, \quad (27)$$

and

$$V_p=\frac{\alpha}{r^4}(1-e^{-(r/r_0)^6}), \quad (28)$$

where $\alpha=0.265$ a.u. is the static dipole polarizability.¹⁴

TABLE II. Configurations included in the diagonalization of the Hamiltonian matrix at different stages of approximation in the nonrelativistic SCW procedure for Al II $1,3F$ states.

Approximation	Configuration
F1	3s(4-14)f
F2	F1 + 3p(3-14)d
F3	F2 + 3p(5-14)g
F4	F3 + 132 other configurations

The empirical formula in Eq. (28) has been employed extensively in other calculations^{5,15,16} to represent the *core dipole polarization interaction*. The cutoff radius $r_0 = 0.79981a_0$ is fitted so that the energy correction due to V_α is equal to the energy difference between the calculated ϵ_{3s} and the observed threshold.^{5,8} This r_0 value is smaller than the one used by Victor *et al.*,¹⁴ partly due to the use of different one-particle Hamiltonians for the orbital wave functions and partly due to the absence of other short-range terms included in the fitted potential in Ref. 14. The value of r_0 would be larger if the calculated ϵ_{nl} for other higher orbits were also fitted to their respective observed thresholds. We should remark at this point that although the calculated energy eigenvalues are affected negligibly by the *dielectric potential* term, our subsequent calculation will show that the influence of this interaction to the state wave functions is one of the most important factors in the correct determination of the fine-structure splittings between different J levels in the 3F manifold.

We will first examine the effect of the configuration interaction to the 1F - 3F term separation following our zeroth-order state wave-function calculation. The calculated term separations for the $3sn$ ($n=4-9$) f configuration series with selected configuration combinations listed in Table II are plotted in Fig. 1, along with the experimental data⁶ and the results from a very elaborate multiconfiguration Hartree-Fock (MCHF) calculation by Froese Fischer.⁴ From the F1 calculation, it is clear that in the *absence* of the configuration interaction from $3p3d$, the calculated 1F - 3F level splittings for the $3snf$ series follows the usual $(n^*)^3$ dependence. When the configuration interactions due to the $3pnd$ series are included (e.g., F2 in Table II), our calculation shows that all members in the $3snf$ 1F series are subject to a net decrease in energy. As for the $3snf$ 3F configuration series, the presence of the $3p3d$ 3F perturber between the $3s6f$ 3F and $3s7f$ 3F states has lowered the energies for the $3s(4-6)f$ 3F states

on the lower-energy side and at the same time raised the energies of the $3sn$ (≥ 7) f 3F states on the higher-energy side.⁵ Therefore the 1F - 3F level inversion can be interpreted qualitatively as the result of the combined effect due to the relatively large energy increase for those neighboring 3F states immediately above the $3p3d$ 3F state and the small energy decrease experienced by their corresponding 1F states. The effect of configuration interaction due to other configuration series is illustrated by F3 and F4 in Fig. 1. Quantitatively, our calculated 1F - 3F term separations shown in Fig. 1 are in close agreement with the experimentally observed values.

Before we present the numerical calculation of the spin-dependent magnetic fine-structure interactions, we will point out an important relationship between the observed level splittings and the calculated zeroth-order state wave functions. As we noted earlier that in the *absence* of significant configuration interaction, the ratio R between level splittings Δ_3 and Δ_2 for each 3F manifold should equal an expected value of 0.75. At first sight, this appears to be inconsistent with the fact that for states (e.g., $3s6f$ 3F and $3p3d$ 3F) which are affected most strongly by the configuration interaction according to the theoretical calculations,^{4,5} their observed ratios R are actually the closest to the value of 0.75. This inconsistency is easily resolved when we examine the contributing radial matrix elements [i.e., Eq. (14)] from the dominating spin-orbit interaction. Our numerical calculation shows that the radial matrix elements for the $l=1$ p orbitals are at least one to two orders of magnitude larger than those of the higher- l orbitals. Consequently, the fact that the value of R for a 3F state is close to 0.75 would merely indicate that the fine-structure-level splitting is actually dominated by the contribution from the $3p3d$ component *alone*, or more specifically, the radial matrix element $\langle 3p | (1/r^3) | 3p \rangle$, when the $3p3d$ contribution to the state wave function is significant. Quantitatively, this link between the level splittings and the probability density of the $3p3d$ component in the state wave functions is shown by Table III. First, we list the ratios of the level splittings Δ_3 and Δ_2 for each of the $3snf$ 3F state to the splittings of the $3p3d$ 3F state. These values are compared with the *relative* probability densities ρ for the $3p3d$ component in the 3F state wave functions. We should note that the $3p3d$ probability density at a maximum value of 36% for the $3p3d$ 3F state⁵ is normalized

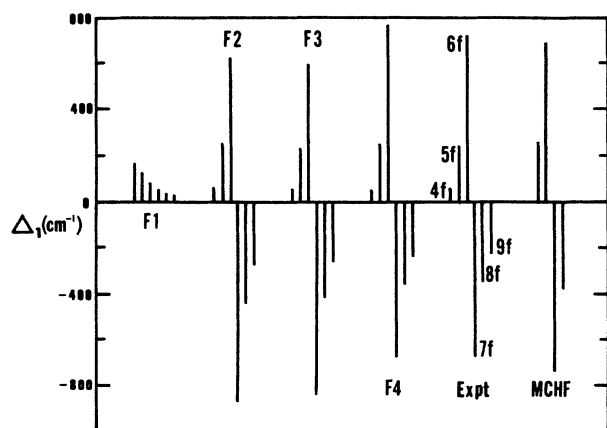


FIG. 1. Comparison between the calculated 1F - 3F electrostatic term separations Δ_1 (in cm^{-1}) with different configuration combinations (i.e., F1-F4 given in Table II) and the experimental 1F_3 - 3F_3 term separations for the $3s(4-9)f$ states. Δ_1 are plotted from left to right for each set of data. The MCHF values for the $3s(5-8)f$ states from Ref. 4 are also plotted from left to right for comparison.

TABLE III. Comparison of the *relative* total probability densities ρ from $3pnd$ components in the state wave functions with the level splittings Δ_2 and Δ_3 for the 3F states. The values of all entries for the $3p3d$ 3F state are *normalized to 1*.

State	Δ_2	Δ_3	With V_d	ρ Without V_d
$3s4f$	0.088	0.078	0.093	0.119
$3s5f$	0.212	0.213	0.226	0.309
$3s6f$	0.694	0.694	0.765	0.996
$3p3d$	1.000	1.000	1.000	1.000
$3s7f$	0.330	0.279	0.317	0.299
$3s8f$	0.102	0.096	0.103	0.104
$3s9f$	0.045	0.043	0.045	0.049

to 1. The close agreement between the relative probability density ρ and the ratios for the level splittings strongly suggests that the multiplet splittings between different J levels are primarily determined by the contribution from the $3p3d$ component in the state wave function.

Although the value of the cutoff radius r_0 does not affect our numerical results noticeably, the need to include the dielectronic interaction V_d discussed earlier is clearly illustrated by the significant difference between the calculated ρ with and without V_d . For states in other quasi-two-electron atoms where the fine-structure splittings are determined by the cancellation between opposite contributions from more than one strongly mixed configurations, the value of the cutoff radius r_0 would become a more sensitive parameter in an accurate determination of the fine-structure splittings. In fact, in addition to the observed energy thresholds, the experimental fine-structure splittings could, in turn, be employed to determine the empirical parameters, such as r_0 , for the core dipole polarization interaction. The result of such a study currently in progress will be reported elsewhere.

The numerical calculations of the spin-dependent magnetic fine-structure interactions are carried out in two stages. First, the Hamiltonian matrix is constructed with states limited to the 3F symmetry. A more complete calculation is carried out in the second stage by including states which consist of at least a non-negligible $3pnd$ component in the state wave function from all other allowed symmetries (i.e., 3G_4 , 1G_4 , and 3F_4 for $J=4$; 3G_3 , 3F_3 , 1F_3 , and 3D_3 for $J=3$; and 3F_2 , 3D_2 , 1D_2 , and 3P_2 for $J=2$) in the construction of the Hamiltonian matrix.

As noted by Blume and Watson,¹² the contribution from the electrons in the 1S core for the spin-orbit and the spin-spin interactions vanishes in the present frozen-core approximation. In addition, as shown by Elliott,^{12,17} the spin-other-orbit interaction between the outer electron in the unfilled shell and electrons in the closed core is equivalent to an effective single-particle spin-orbit interaction for the outer electron, and as a result effectively reduces the nuclear charge Z experienced by the outer electrons. Consequently, in practice, for the spin-other-orbit interaction $H_{s.o.o.}$, the sum over all i and j in Eq. (4) may be replaced by a single term limited to two outer electrons if the nuclear charge Z is replaced by an effective charge Z_{eff} in the spin-orbit interaction $H_{s.o.}$ in Eq. (2). In the present calculation, values of $Z_{\text{eff}}=11.4$ for the p orbitals, $Z_{\text{eff}}=7.4$ for the d orbitals, and $Z_{\text{eff}}=3$ for all higher- l orbitals are selected for the best fit¹⁸ to the experimental level splittings.

In contrast to the positive Z_{eff} for the d orbitals used in the present study, Laughlin and Victor¹⁸ had introduced a negative Z_{eff} so that the inverted fine-structure splittings for the 2D series in Mg II and the 3D series in Mg I might be fitted simultaneously with the same negative Z_{eff} for the d orbitals. For the 2D series along the Na isoelectronic sequence, instead of the use of a fitted result in a lowest-order nonrelativistic central-field approximation with a negative Z_{eff} ,¹⁸ more elaborate theoretical studies^{19,20} have concluded that the level inversion is caused by a negative contribution due to the interference

between the spin-orbit interaction and the electrostatic exchange interaction of the p and d electron and, to the order of α^2 , it is equivalent to a first-order calculation in the relativistic central-field approximation including a core polarization interaction, such as the one given by Eq. (28), if the electrostatic exchange interaction is properly taken into account.¹⁵ As for the Mg 3D series, a negative contribution due to the $\langle 3p | (1/r^3) | 3p \rangle$ term from the small but finite $3pnf$ components in the $3snd$ 3D state wave function could be comparable in magnitude to the positive contribution from the $3snd$ component when a smaller positive Z_{eff} is used for the d orbitals. A negative $3pnf$ contribution could conceivably lead to the level inversion if its magnitude is larger than the positive $3snd$ contribution. Moreover, the combined negative $3pnf$ contribution and the negative $3snd$ contribution due to a negative Z_{eff} for the d orbitals might have been responsible for the consistently larger level splittings found in the calculated values than that of the observed ones reported by Laughlin and Victor.¹⁸ The cancellation between the positive and negative contributions of similar magnitude could also enhance the effect due to the small mixing with other LS states as well as the spin-spin and spin-other-orbit interactions. As a result, the ratio R deviates noticeably from the Landé interval rule. Again, a negative Z_{eff} is not required to account for the inverted 3D series.

The calculated level splittings Δ_2 and Δ_3 following the second diagonalization of the Hamiltonian matrices are shown in Figs. 2 and 3. We should point out that in the absence of any mixing with the $3p3d$ configuration, the individual contribution from the $3snf$ configuration to the Δ_2 and Δ_3 alone is about two to three orders of magnitude smaller than those shown in Figs. 2 and 3. The calculated ratios R between level splittings are shown in Fig. 4. Again, the results from the present calculation

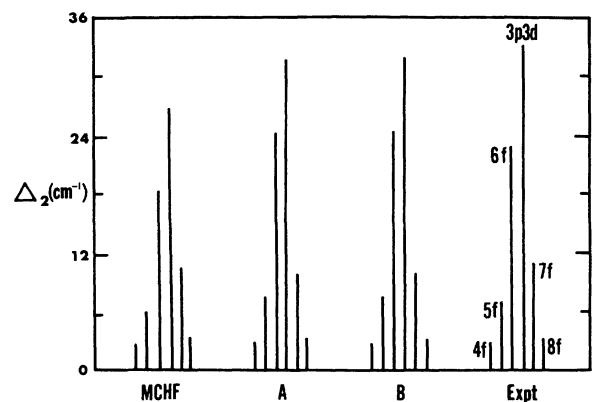


FIG. 2. Comparison between the calculated 3F_4 - 3F_3 level splittings Δ_2 in cm^{-1} and the experimental data. Data set A denotes the calculation in that only states with 3F symmetry are included and B denotes the calculation in that states with all allowed symmetries (i.e., 3F_3 , 1F_3 , 3D_3 , and 3G_3 in $J=3$ and 3F_4 , 1G_4 , and 3G_4 in $J=4$) are included in the second diagonalization. The MCHF results from Ref. 4 are also included for comparison. The splittings for $3s4f$, $3s5f$, $3s6f$, $3p3d$, $3s7f$, and $3s8f$ states are plotted from left to right for each data set.

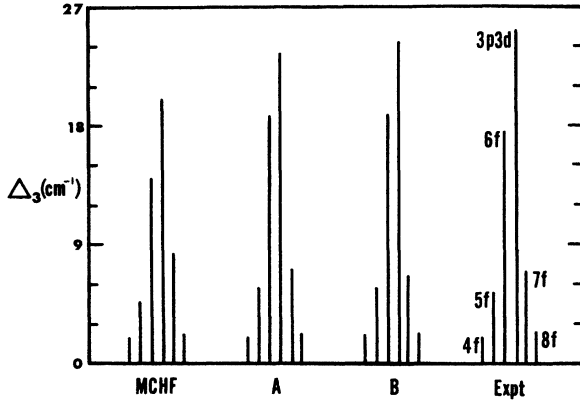


FIG. 3. Comparison between the calculated 3F_3 - 3F_2 level splittings Δ_3 in cm^{-1} and the experimental data. Data set *A* denotes the calculation in that only states with 3F symmetry are included and *B* denotes the calculation in that states with all allowed symmetries (i.e., 3F_3 , 1F_3 , 3D_3 , and 3G_3 in $J=3$ and 3F_2 , 3D_2 , 1D_2 , and 3P_2 in $J=2$) are included in the second diagonalization. The MCHF results from Ref. 4 are also included for comparison. The splittings for $3s4f$, $3s5f$, $3s6f$, $3p3d$, $3s7f$, and $3s8f$ states are plotted from left to right for each data set.

are in close agreement with the experimental data. The MCHF results⁴ are also shown for comparison. It is interesting to note that whereas the absolute level splittings are not affected noticeably by the addition of states from other symmetries, the calculated ratios R between Δ_3 and Δ_2 are affected significantly. In particular, the calculated value of R for $3s7f$ 3F state is found to be in much closer agreement with the experimental value when additional states of other symmetries are included. Finally, we note that the contributions from the spin-other-orbit and the spin-spin interactions are substantially smaller than the spin-orbit interaction, except for the lowest $3s4f$ states, in that the splittings due to the spin-orbit interaction are relatively small compared with other states whereas the spin-other-orbit interaction is at its maximum. In summary, the direct link between the fine-structure-level splittings and the probability densities of the dominating configuration in state wave functions identified in the

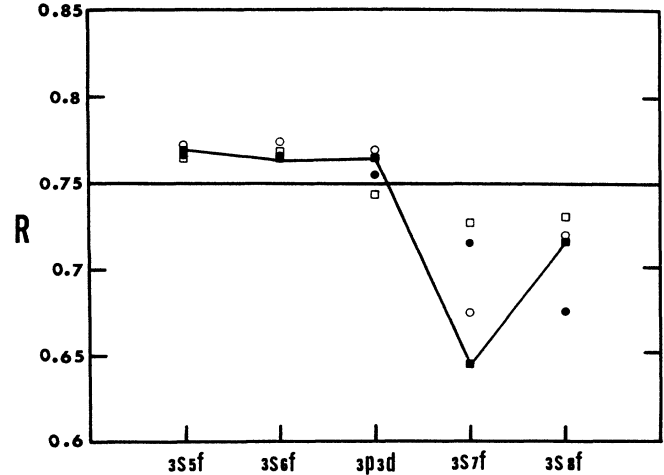


FIG. 4. The ratio between fine-structure-level splittings, i.e., $R = \Delta_3/\Delta_2$. A value of 0.75 is expected from the *Landé interval rule*. The values of R are given for experimental data (■), calculation including 3F states only (□), calculation including states with all allowed symmetries (○), and MCHF values from Ref. 4 (●).

present study has added to the experimental determination of fine-structure-level splittings for states dominated by configuration interaction, a potentially promising dimension in the understanding of the effect of configuration interaction in a quasi-two-electron atom.

ACKNOWLEDGMENT

This work is supported by the National Science Foundation under Grant No. PHY-84-08333.

APPENDIX

With the spin-spin interaction expressed as a scalar product of tensor operators given by Eq. (15), the matrix elements between configuration wave functions in J representation can be derived analytically following a straightforward application of the Wigner-Eckart theorem, i.e.,

$$\begin{aligned} \langle \Psi_{n_\alpha l_\alpha n_\beta l_\beta}^{S'LJM'} | H_{ss} | \Psi_{n_\mu l_\mu n_\nu l_\nu}^{SLJM} \rangle &= \delta_{J'J} \delta_{M'M} \delta_{S'S'} \delta_{S_1 S_1'} (5^{1/2}/2) \\ &\times \sum_k (-1)^k \left[\frac{(2k+5)!}{(2k)!} \right]^{1/2} [X(\alpha\beta\mu\nu L'LJ; k, k+2) + (-1)^\Delta X(\alpha\beta\nu\mu L'LJ; k, k+2)], \end{aligned} \quad (\text{A1})$$

where the phase factor Δ is the same as the one given in Eq. (10) and

$$X(\alpha\beta\mu\nu L'LJ; \lambda, \tau) = F(\alpha\mu\lambda, \beta\nu\tau; L'LJ) R_2^\lambda(\alpha\beta\mu\nu) + F(\alpha\mu\tau, \beta\nu\lambda, L'LJ) R_1^\lambda(\alpha\beta\mu\nu). \quad (\text{A2})$$

The angular factor F is given by

$$F(\alpha\mu\lambda, \beta\nu\tau; L'LJ) = (-1)^L + J [(2L'+1)(2L+1)]^{1/2} (l_\alpha \| C^{(\lambda)} \| l_\mu) (l_\beta \| C^{(\tau)} \| l_\nu) \begin{Bmatrix} L' & L & 2 \\ 1 & 1 & J \end{Bmatrix} \begin{Bmatrix} l_\alpha & l_\mu & \lambda \\ l_\beta & l_\nu & \tau \\ L' & L & 2 \end{Bmatrix}, \quad (\text{A3})$$

where the reduced matrix element of the spherical harmonic $C^{(k)}$ is given by²¹

$$(l \| C^{(k)} \| l') = (-1)^l [(2l+1)(2l'+1)]^{1/2} \begin{pmatrix} l & k & l' \\ 0 & 0 & 0 \end{pmatrix}. \quad (\text{A4})$$

The radial integrals R_1 and R_2 are given by

$$R_1^k(\alpha, \beta, \mu, \nu) = \int_0^\infty ds \chi_{n_\alpha l_\alpha}(s) \chi_{n_\mu l_\mu}(s) \frac{1}{s^{k+3}} \int_0^s dr r^k \dot{\chi}_{n_\beta l_\beta}(r) \chi_{n_\nu l_\nu}(r) \quad (\text{A5})$$

and

$$R_2^k(\alpha, \beta, \mu, \nu) = \int_0^\infty ds \chi_{n_\alpha l_\alpha}(s) \chi_{n_\mu l_\mu}(s) s^k \int_s^\infty dr \frac{1}{r^{k+3}} \chi_{n_\beta l_\beta}(r) \chi_{n_\nu l_\nu}(r). \quad (\text{A6})$$

A change of order of integration will immediately lead to a simple relationship between these two radial integrals, i.e.,

$$R_1^k(\alpha, \beta, \mu, \nu) = R_2^k(\beta, \alpha, \nu, \mu). \quad (\text{A7})$$

Similarly, with the spin-other-orbit interaction expressed as the sum of scalar products of tensor operators given by Eq. (23), the matrix elements can be evaluated with a lengthy but straightforward application of the Wigner-Eckart theorem. Finally, we obtain the following analytical expression:

$$\begin{aligned} \langle \Psi_{n_\alpha l_\alpha n_\beta l_\beta}^{S'L'J'M'} | H_{\text{s.o.o.}} | \Psi_{n_\mu l_\mu n_\nu l_\nu}^{SLJM} \rangle &= \delta_{J'J} \delta_{M'M} (-1)^{L+J} [2 + (-1)^{S+S'}] \rho(L'S', LS, J) \\ &\times \sum_{k=0}^{\infty} [\omega_k(\alpha\beta L', \mu\nu L; k+1) + (-1)^\Delta \omega_k(\alpha\beta L', \nu\mu L; k+1) \\ &\quad + (-1)^{\Delta'} \omega_k(\beta\alpha L', \mu\nu L; k+1) + (-1)^{\Delta+\Delta'} \omega_k(\beta\alpha L', \nu\mu L; k+1) \\ &\quad + \eta_k(\alpha\beta L', \mu\nu L) + (-1)^\Delta \eta_k(\alpha\beta L', \nu\mu L)], \end{aligned} \quad (\text{A8})$$

where

$$\omega_k(\alpha\beta L', \mu\nu L; \lambda) = T_k(\alpha\beta L', \mu\nu L; \lambda) + \xi_k(\alpha\beta L', \mu\nu L), \quad (\text{A9})$$

$$T_k(\alpha\beta L', \mu\nu L; \lambda) = f_k(\alpha\beta L', \mu\nu L; \lambda) [(k+1)R_1^{k+1}(\alpha\beta\mu\nu) - (k+2)R_2^{k-1}(\alpha\beta\mu\nu)], \quad (\text{A10})$$

$$\xi_k(\alpha\beta L', \mu\nu L) = (2k+1)f_k(\alpha\beta L', \mu\nu L; k)R_1^k(\alpha\beta\mu\nu) - (2k+5)f_k(\alpha\beta L', \mu\nu L; k+2)R_2^k(\alpha\beta\mu\nu), \quad (\text{A11})$$

$$f_k(\alpha\beta L', \mu\nu L; \lambda) = (-1)^k (2k+3) (l_\mu \| l^{(1)} \| l_\mu) (l_\alpha \| C^{(\lambda)} \| l_\mu) (l_\beta \| C^{(\lambda)} \| l_\nu) \begin{Bmatrix} \lambda & 1 & k+1 \\ l_\mu & l_\alpha & l_\mu \end{Bmatrix} \begin{Bmatrix} l_\alpha & l_\mu & k+1 \\ l_\beta & l_\nu & \lambda \\ L' & L & 1 \end{Bmatrix}, \quad (\text{A12})$$

$$\eta_k(\alpha\beta L', \mu\nu L) = g_k(\alpha\beta L', \mu\nu L) \{ R_1^k(\alpha\beta\bar{\mu}\nu) + R_2^{k-2}(\alpha\beta\bar{\mu}\nu) - (-1)^{S+S'} [R_1^k(\beta\alpha\bar{\nu}\mu) + R_2^{k-2}(\beta\alpha\bar{\nu}\mu)] \}, \quad (\text{A13})$$

and

$$g_k(\alpha\beta L', \mu\nu L) = (-1)^{k+1} [k(k+1)(2k+1)]^{1/2} (l_\alpha \| C^{(k)} \| l_\mu) (l_\beta \| C^{(k)} \| l_\nu) \begin{Bmatrix} l_\alpha & l_\mu & k \\ l_\beta & l_\nu & k \\ L' & L & 1 \end{Bmatrix}. \quad (\text{A14})$$

The expressions for the angular factor ρ and the phases Δ and Δ' are the same as those given earlier. The bar on the top of the arguments, e.g., $\bar{\mu}$, in the radial integrals R_1 and R_2 in Eq. (A13) indicates that the radial wave functions $\chi_{n_\mu l_\mu}(r)$ should be replaced by

$$r \left[\frac{\partial}{\partial r} [\chi_{n_\mu l_\mu}(r)/r] \right].$$

- ¹I. I. Sobel'man, *Introduction to the Theory of Atomic Spectra* (Pergamon, New York, 1972).
- ²H. A. Bethe and E. E. Salpeter, *Quantum Mechanics of One- and Two-electron Atoms* (Springer-Verlag, Berlin, 1957).
- ³A. W. Weiss, *Phys. Rev. A* **9**, 1524 (1974).
- ⁴C. Froese Fischer, *Phys. Scr.* **21**, 466 (1980).
- ⁵T. N. Chang and R. Wang, *Phys. Rev. A* **36**, 3535 (1987).
- ⁶W. C. Martin and R. Zalubas, *J. Phys. Chem. Ref. Data* **8**, 817 (1979); V. Kaufman and L. Hagan, *J. Opt. Soc. Am.* **69**, 232 (1979).
- ⁷R. N. Zare, *J. Chem. Phys.* **45**, 1966 (1966).
- ⁸T. N. Chang and Y. S. Kim, *Phys. Rev. A* **34**, 2609 (1986).
- ⁹T. N. Chang, *Phys. Rev. A* **34**, 4550 (1986).
- ¹⁰H. H. Marvin, *Phys. Rev.* **71**, 102 (1947).
- ¹¹B. R. Judd, *Operator Techniques in Atomic Spectroscopy* (McGraw-Hill, New York, 1963).
- ¹²M. Blume and R. E. Watson, *Proc. R. Soc. London, Ser. A* **270**, 127 (1962).
- ¹³C. Bottcher and A. Dalgarno, *Proc. R. Soc. London, Ser. A* **340**, 187 (1974).
- ¹⁴G. A. Victor, R. F. Stewart, and C. Laughlin, *Astrophys. J., Suppl. Ser.* **31**, 237 (1976).
- ¹⁵E. Luc-Koenig, *Phys. Rev. A* **13**, 2114 (1976).
- ¹⁶K. Bartschat, M. R. H. Rudge, and P. Scott, *J. Phys. B* **19**, 2469 (1986).
- ¹⁷J. P. Elliott, *Proc. R. Soc. London, Ser. A* **218**, 345 (1953).
- ¹⁸C. Laughlin and G. A. Victor, *Astrophys. J.* **192**, 551 (1974).
- ¹⁹I. Holmgren, I. Lindgren, J. Morrison, and A.-M. Martensson, *Z. Phys.* **276**, 179 (1976).
- ²⁰R. M. Sternheimer, J. E. Rodgers, and T. P. Das, *Phys. Rev. A* **17**, 505 (1978).
- ²¹A. R. Edmonds, *Angular Momentum in Quantum Mechanics* (Princeton University Press, Princeton, NJ, 1957).